



Published in final edited form as:

J Med Genet. 2020 June ; 57(6): 371–379. doi:10.1136/jmedgenet-2019-106333.

Increased *TBX6* Gene Dosages Induce Congenital Cervical Vertebral Malformations in Humans and Mice

Xiaojun Ren^{1,2}, Nan Yang^{1,2,3}, Nan Wu^{4,5,6,7}, Ximing Xu⁸, Weisheng Chen^{4,5}, Ling Zhang^{1,2}, Yingping Li¹, Renqian Du⁷, Shuangshuang Dong^{1,2}, Sen Zhao^{4,5}, Shuxia Chen¹, Li-Ping Jiang⁹, Lianlei Wang^{4,5}, Jianguo Zhang^{4,5,6}, Zhihong Wu^{4,5,10}, Li Jin¹, Guixing Qiu^{4,5,6}, James R. Lupski^{7,11,12}, Jianguo Shi^{8,*}, Feng Zhang^{1,2,3,*}, Pengfei Liu^{7,13}

¹Obstetrics and Gynecology Hospital, NHC Key Laboratory of Reproduction Regulation (Shanghai Institute of Planned Parenthood Research), State Key Laboratory of Genetic Engineering at School of Life Sciences, Fudan University, Shanghai 200011, China

²Shanghai Key Laboratory of Female Reproductive Endocrine Related Diseases, Shanghai 200011, China

³State Key Laboratory of Reproductive Medicine, Center for Global Health, School of Public Health, Nanjing Medical University, Nanjing 211166, China

⁴Department of Orthopedic Surgery, Peking Union Medical College Hospital, Peking Union Medical College and Chinese Academy of Medical Sciences, Beijing 100730 China

⁵Beijing Key Laboratory for Genetic Research of Skeletal Deformity, Peking Union Medical College and Chinese Academy of Medical Sciences, Beijing 100730, China

⁶Medical Research Center of Orthopedics, Chinese Academy of Medical Sciences, Beijing 100730, China

⁷Department of Molecular and Human Genetics, Baylor College of Medicine, Houston, TX 77030, USA

⁸Department of Orthopedic Surgery, Spine Center, Changzheng Hospital, Second Military Medical University, Shanghai 200003, China

⁹State key Laboratory of Molecular Engineering of Polymers, Department of Macromolecular Science, Fudan University, Shanghai 200011, China

¹⁰Department of Central Laboratory, Peking Union Medical College Hospital, Peking Union Medical College and Chinese Academy of Medical Sciences, Beijing 100730, China

¹¹Department of Pediatrics, Baylor College of Medicine, Houston, TX 77030, USA

*Correspondence to Jianguo Shi, changzhengspine@smmu.edu.cn and Feng Zhang, zhangfeng@fudan.edu.cn.

XR, NY and NW contributed equally.

JS, FZ and PL contributed equally.

Contributors

XR, NY, NW and FZ designed the study. XR, NY, NW, XX, WC, LZ, YL, RD, SD, SZ, SC, L-PJ and LW conducted experiments. XR, NY, NW, XX, WC, LZ, YL, RD, SD, SZ, SC, L-PJ, LW, JZ, ZW, LJ, GQ, JRL, JS, FZ and PL analysed data. XR, NY, NW, JRL, JS, FZ and PL wrote the manuscript. JS, FZ and PL supervised the study.

Ethics approval

Declaration of Helsinki and approved by the Ethical Committees of the centers participating in this study.

¹²Texas Children's Hospital, Houston, TX 77030, USA

¹³Baylor Genetics, Houston, TX 77021, USA

Abstract

Background—Congenital vertebral malformations (CVMs) manifest with abnormal vertebral morphology. Genetic factors have been implicated in CVM pathogenesis, but the underlying pathogenic mechanisms remain unclear in most subjects. We previously reported that the human 16p11.2 BP4-BP5 deletion and its associated *TBX6* dosage reduction caused CVMs. We aim to investigate the reciprocal 16p11.2 BP4-BP5 duplication and its potential genetic contributions to CVMs.

Methods and Results—Patients who were found to carry the 16p11.2 BP4-BP5 duplication by chromosomal microarray analysis were retrospectively analyzed for their vertebral phenotypes. The spinal assessments in seven duplication carriers showed that four (57%) presented characteristics of CVMs, supporting the contention that increased *TBX6* dosage could induce CVMs. For further *in vivo* functional investigation in a model organism, we conducted genome editing of the upstream regulatory region of mouse *Tbx6* using CRISPR-Cas9, and obtained three mouse mutant alleles (*Tbx6^{up1}* to *Tbx6^{up3}*) with elevated expression levels of *Tbx6*. Luciferase reporter assays showed that the *Tbx6^{up3}* allele presented with the 160% expression level of that observed in the reference (+) allele. Therefore, the homozygous *Tbx6^{up3/up3}* mice could functionally mimic the *TBX6* dosage of heterozygous carriers of 16p11.2 BP4-BP5 duplication (approximately 150%, i.e. 3/2 gene dosage of the normal level). Remarkably, 60% of the *Tbx6^{up3/up3}* mice manifested with CVMs. Consistent with our observations in humans, the CVMs induced by increased *Tbx6* dosage in mice mainly affected the cervical vertebrae.

Conclusion—Our findings in humans and mice consistently support that an increased *TBX6* dosage contributes to the risk of developing cervical CVMs.

INTRODUCTION

Congenital vertebral malformations (CVMs) are structural deformities of the vertebrae that are caused by abnormal somitogenesis during embryogenesis. CVMs can result in an abnormal appearance, impaired functions of the heart and lungs, back pain, and disability.^{1,2} The overall morbidity of CVMs is reported to be 0.5 – 1 per 1000 live births, which seriously affects human health.^{3,4} Although various factors have been implicated in inducing CVM, the etiologies and underlying biology of specific subtypes of CVMs remain poorly understood.¹

Genetic factors play important roles in human congenital diseases. Copy number variants (CNVs), including genomic deletions and duplications, can be generated from DNA rearrangements (online supplementary figure 1), and are responsible for a major class of human conditions termed genomic disorders.^{5,6} The deletion of approximately 600 kb 16p11.2 BP4-BP5 region has been demonstrated to be associated with CVMs in human subjects.^{7,8,9} The presumed pathogenic mechanism of deletion CNVs is dosage insufficiency of critical development-associated genes in the affected region.^{10,11,12,13} Such critical gene dosages and expression levels may be relevant to birth defects potentially relating to

developmental windows of gene expression or expression gradients required for tissue differentiation during development. *TBX6* (MIM: 602427), mapping in the human proximal 16p11.2 BP4-BP5 region (online supplementary figure 1A), has been pinpointed as the gene responsible for the observed CVMs in 16p11.2 BP4-BP5 deletion carriers.^{9,14,15,16,17}

A pair of directly-oriented genomic repeats located in human 16p11.2 can mediate the recurrent 16p11.2 BP4-BP5 deletion via non-allelic homologous recombination (online supplementary figure 1B).^{18,19} The same mutational mechanism can also generate the reciprocal 16p11.2 BP4-BP5 duplication. The frequencies of 16p11.2 BP4-BP5 CNVs vary in different reports; the CNV frequency in the combined population cohorts is approximately 0.04% for deletion, and 0.05% for duplication.^{20,21} The gene dosage of *TBX6* is reduced (from two copies to one copy) in 16p11.2 BP4-BP5 deletion carriers, whereas the *TBX6* dosage is increased (from two copies to three copies) by 16p11.2 BP4-BP5 duplication (online supplementary figure 1) – a reciprocal gene dosage that could potentially cause a mirror trait.²²

The dosages of the genes mapping within the 16p11.2 BP4-BP5 region are altered due to CNVs, and there are mirror phenotypes among human subjects harboring the 16p11.2 BP4-BP5 deletion or reciprocal duplication. The clinical features of individuals with 16p11.2 BP4-BP5 deletion have been described mostly for those with abnormal developmental, neuropsychological and metabolic phenotypes such as head circumference (macrocephaly), brain structures, face morphology, autism, schizophrenia and obesity.^{23,24,25,26,27,28} In contrast, 16p11.2 BP4-BP5 duplication preserves the mirror effects of gene dosage changes, and thus results in mirror phenotypes (microcephaly, underweight and etc.).^{20,29,30,31} Meanwhile, some of these mirror trait phenotypes associated with this and other loci have been illuminated by mouse models.^{32,33,34,35} Among these mirror traits, some are related to the bone formation and morphological phenotypes. Therefore, considering our gene dosage and expression compound inheritance model and confirmed pathogenesis of the 16p11.2 BP4-BP5 deletion in CVMs,^{9,14,15} we hypothesized that human 16p11.2 BP4-BP5 duplication may induce CVMs due to the increased gene dosage of *TBX6*. Some reports indicate that individuals with the 16p11.2 BP4-BP5 duplications may manifest scoliosis among other clinical phenotypes.^{23,36} Though a previous report showed that 21 out of 270 carriers of 16p11.2 BP4-BP5 duplication manifest with scoliosis,³⁷ the exact correlation between 16p11.2 BP4-BP5 duplication and the position or incidence of CVMs has not been established nor systematically investigated.

Here, we retrospectively analyzed vertebral morphology in human subjects with 16p11.2 BP4-BP5 duplication and generated mouse models via CRISPR-Cas9 to investigate the potential genetic contribution of increased *TBX6* dosage to vertebral malformation *in vivo*. Our data strongly support a gene dosage model for cervical CVMs.

METHODS

Human subjects with 16p11.2 BP4-BP5 duplication

We analyzed clinical data of the subjects with 16p11.2 BP4-BP5 duplications from Baylor Genetics (BG; Houston, USA). These subjects were initially investigated by clinical

chromosomal microarray analysis (CMA; Agilent Technologies Inc., Santa Clara, USA) due to various medical problems. DNA samples were extracted from the peripheral blood. Procedures for the DNA extraction, digestion, labeling and hybridization for CMA were followed by the manufactures' instructions.^{38,39,40} The algorithm requires at least three consecutive probes with the \log_2 ratio value > 0.4 to detect a duplication. The clinical diagnoses of CVMs were confirmed by radiological imaging. Every image was carefully evaluated independently by three orthopedists. A diagnosis of CVM was made only when all the three orthopedists unanimously agreed on the diagnosis. The Sanger sequencing of "T-C-A" haplotypes was conducted as per our previous report.⁹

Mouse strains and animal husbandry

The C57BL/6J background strain was adopted in all mouse experiments. All mice were housed in a specific pathogen-free (SPF) barrier facility. To investigate the vertebral phenotypes in mice, age- and sex- matched wild type mice and *Tbx6*-mutated mice were housed under controlled light-cycle illumination (6:00-18:00), moisture (40%-70%) and temperature (21°C to 23°C). Every littermate was separated at the age of four weeks and the numbers of mice housed per cage were controlled below six in every cage. All experiments involving mice were performed according to the guideline for the Care and Use of Laboratory Animals of the US National Institutes of Health. This study was approved by the Animal Ethics Committee at the School of Life Science, Fudan University.

Genomic editing using CRISPR-Cas9

To obtain the specific sgRNA and target sites of our interest, we used the online CRISPR Design Tool (<http://tools.genome-engineering.org>).⁴¹ Online supplementary table 1 shows the target sequences of sgRNA in the mouse genome. Every step was carried out by standard procedures with minimal modification. The zygotes from C57BL/6J strain mice (200 cells for each RNA) were injected with sgRNA and Cas9 mRNA (10 ng/ μ l for each RNA).⁴² Offspring (F1) was obtained by the founder (F0) mice crossing with wild type C57BL/6J mice. Genomic DNAs from toe clips were genotyped by PCR and Sanger sequencing. Online supplementary table 2 shows the PCR primers used for amplification and sequencing.

Cell culture and *in vitro* transcription assay

To construct reporter plasmids, we amplified the 992 bp DNA fragments that included the potential regulatory elements of mouse *Tbx6*. Online supplementary table 3 shows the primers for amplification. The fragments containing the wild type and potential hypermorphic alleles of *Tbx6* were respectively constructed into the PGL3-Basic vector (Promega) enabling fusion to the reporter gene. The P19CL6 cell line (kindly provided by Prof. Yunzeng Zou, Fudan University, China) was derived from mouse embryonal carcinoma cells.⁴³ The expression of TBX6 protein could be induced during differentiation of P19CL6 cells.⁴⁴ The P19CL6 cells were grown in α -MEM (Gibco) containing 10% fetal bovine serum (Gibco) and remained at 37°C and in 5% carbon dioxide. After digestion by trypsin, 1×10^5 cells were seeded to a 24-well plate with 500 μ l culture medium with 1% DMSO (Sigma).^{42,43} After 24 hours culture, cells were transfected with 500 ng plasmids of each promoter fused with firefly luciferase reporter plasmid and 50 ng pRL-TK plasmid as a normalizing control using Lipofectamine 3000 (Invitrogen). After 24 hours culture,

cells were lysed and 25 μ l of supernatant was used to assay the luciferase activity using the Dual-Luciferase Reporter Assay System (Promega). The relative reporter activity was normalized by the firefly activity to Renilla activity. Each assay was performed with at least three replicates.

Whole-mount RNA *in situ* hybridization in embryos

Embryos were dissected at E9.5 (the day of plugs is E0.5), fixed in 4% paraformaldehyde overnight at 4°C, washed in PBST (PBS contain 0.1% tween-20), and dehydrated through a series of methanol/PBST (25%, 50%, 75% and 100%). Embryos were stored in pure methanol at -80°C. Every step was carried out by standard procedures.⁴⁵ Embryos were treated with proteinase K (10 μ g/ml in PBST) for 10 minutes without rotation at room temperature. The concentration of the probe in the hybridization solution is 1 ng/ μ l. Probes, bounded with digoxigenin, were detected by alkaline phosphatase conjugated anti-digoxigenin antibodies (Roche, Germany).

Real-time quantitative PCR

The total RNA of the caudal part of embryos was extracted with Trizol reagent (Ambion) and reversely transcribed into cDNAs with HiScript II Q RT SuperMix (Vazyme). The obtained cDNAs were respectively diluted 5-fold to be used in the following real-time quantitative PCR (qPCR) with AceQ qPCR SYBR Green Master Mix (Vazyme). The expression of mRNA was quantified according to the 2^{-Ct} method, and the dosage of *Tbx6* was normalized by the internal control of *Gapdh*. The primers for *Tbx6* and *Gapdh* were as shown in online supplementary table 4.

Vertebral analysis

Mice (aged from 35 to 45 days) were examined using micro-computed tomography (micro-CT). The wild type and mutant groups were sex-matched, and the amounts of males and females were totally the same in each group. Micro-CT imaging of the vertebrae was performed using the SkyScan scanner (SkyScan 1176, Bruker). Anesthesia was delivered to mice via the intraperitoneal injection of 2% pelltobarbitalum Natricum (dissolved in normal saline, 5ml/kg by body weight). The vertebrae were scanned with the following setting parameters: 50 KV for X-ray tube voltage, 497 μ A for X-ray tube current, 35 μ m for pixel resolution, 2° for rotation steps, and 360° rotation around the vertical axis.¹⁴ Acquired X-ray projections were reconstructed using the SkyScan NRecon software with 33% bean-hardening, and the value of smoothing, misalignment and ring is 2, 1 and 6, respectively.

Statistical analysis

Statistical differences between groups in the luciferase experiment and qPCR assays were evaluated with the unpaired *t* test. The Fisher's exact test was adopted in the micro-CT analysis. A two-sided $P < 0.05$ is considered statistically significant. All statistical procedures were carried out using GraphPad Prism5. *, **, *** and **** denote P values of < 0.05 , < 0.01 , < 0.001 and < 0.0001 , respectively.

RESULTS

Increased risk of CVMs in human subjects with 16p11.2 BP4-BP5 duplication

To investigate the potential involvement of human 16p11.2 BP4-BP5 duplication in CVMs, we retrospectively reviewed the subjects with the 16p11.2 BP4-BP5 duplication from a large cohort of patients that were tested clinically by CMA due to various medical problems.^{46,47} The spinal X-ray images were available for seven 16p11.2 BP4-BP5 duplication carriers (figure 1A). The diagnosed age of these seven subjects ranged from 9 months to 16 years old. As shown in table 1, four (57%) of these human subjects with 16p11.2 BP4-BP5 duplication presented with CVMs. Subjects BD01 and BD05 manifested with formation failures in vertebrae C6 and C7; BD13 manifested with formation failures in C5 and C6; BD24 has extensive failure of formations in the vertebral plates from C3 to T7 (figure 1B, table 1 and online supplementary figure 2).

To further investigate the potential increased risk of CVMs in the human carriers of 16p11.2 BP4-BP5 duplication, the previously reported prevalence rates of CVMs in two large populations were employed as controls: a study of CVMs by chest minifilms in general populations (frequency of CVM: 7/15000) and a study of scoliosis in Singapore school children (frequency of CVM/congenital scoliosis: 12/55747).^{4,48} Notably, 16p11.2 BP4-BP5 duplication carriers seem to have a significantly higher risk of CVMs (4/7 VS 7/15000, $P < 0.0001$, OR = 2856, 95% CI of OR: 629 to 12865, by the Fisher's exact test when taking the general population as a control; 4/7 VS 12/55747, $P < 0.0001$, OR = 6193, 95% CI of OR: 1443 to 26474, by the Fisher's exact test when taking the Singapore school children as controls).

Mouse mutants with increased *Tbx6* expression

The *TBX6* gene in the human 16p11.2 BP4-BP5 region has been demonstrated to be responsible for the observed CVMs in 16p11.2-deletion carriers. We hypothesize that the increased expression of dosage-sensitive *TBX6* may also cause a predisposition to CVMs in subjects with 16p11.2 BP4-BP5 duplication. To generate a mouse model for functionally mimicking the increased dosage of *TBX6* in human 16p11.2 BP4-BP5 duplication carriers, we genetically modified the upstream regions of mouse *Tbx6*, where polymorphic noncoding common variant alleles are known to modulate *Tbx6* expression.¹⁴ We employed the CRISPR-Cas9 technology to generate mouse models with increased *Tbx6* expression *in vivo*. Genomic editing was conducted in the upstream, conserved noncoding region of *Tbx6* (figure 2A) in C57BL/6J mice.⁴² Ten *Tbx6* mutants were generated, and their genotypes were confirmed by Sanger sequencing (online supplementary figure 3).

The *Tbx6* expression levels of these mutants were evaluated by luciferase reporter assays in P19CL6 cells.⁴⁴ Three mutants, named *Tbx6^{up1}*, *Tbx6^{up2}*, and *Tbx6^{up3}*, demonstrated increased *Tbx6* expressions (figure 2B). These three mutants carried short deletions, ranging from 7 to 47 base pairs (bp) in length, in the upstream sequence of *Tbx6* (figure 2B). The expression level of the *Tbx6^{up3}* allele was approximately 160% of that in the wild-type allele ($P < 2.2 \times 10^{-9}$, *t* test) (figure 2C). It was previously reported that the increased *TBX6* expression in human 16p11.2 BP4-BP5 duplication carriers was 150% of that in control

subjects.⁴⁹ Thus, the *Tbx6*^{up3/up3} mice could closely recapitulate the gene dosage/expression change for *TBX6* occurring with heterozygous duplications in the 16p11.2 BP4-BP5 region. The mutated sequence in *Tbx6*^{up3/up3} mice was confirmed by Sanger sequencing (online supplementary figure 4).

To further confirm the contention that the *Tbx6*^{up3/up3} mice presented increased *Tbx6* expression *in vivo*, we conducted whole-mount RNA *in situ* hybridization in E9.5 embryos.⁵⁰ As expected, the increased *Tbx6* expression was observed in *Tbx6*^{up3/up3} embryos (figure 3). Meanwhile, the qPCR data also indicate that there is an elevation of *Tbx6* expression in *Tbx6*^{up3/up3} mouse embryos (online supplementary figure 5).

Dosage sensitivity of increased mouse *Tbx6* expression predisposed to CVMs

To investigate the phenotypic consequence of increased dosage of mouse *Tbx6*, we compared the *Tbx6*^{+/+} (wild type) and *Tbx6*^{up3/up3} mice on the C57BL/6J background, and examined vertebral phenotypes of the adult mice (aged from 35 to 45 days, each group has 20 mice) using micro-CT. The *Tbx6*^{up3/up3} mice presented with an increased risk of developing CVMs. No obvious CVMs were observed in *Tbx6*^{up1/up1} and *Tbx6*^{up2/up2} mice. In total, 12 (60%) out of 20 *Tbx6*^{up3/up3} mice developed CVMs, and the rate was significantly higher ($P < 4.4 \times 10^{-4}$, Fisher's exact test) than that of the wild-type mice (1/20, 5%, figure 4). The morphological vertebral defects observed in the *Tbx6*^{up3/up3} mice included fusions and clefts of the vertebrae (figure 4B). Our observations in mice suggest that the dosage sensitivity of increased *Tbx6*/*TBX6* expression is associated with an increased incidence of CVMs.

Localized cervical CVMs in both human subjects and the mouse model with increased *TBX6*/*Tbx6* dosage

Among these four patients with 16p11.2 BP4-BP5 duplication and CVMs, all the CVM defects were localized to the cervical segments from vertebrae C3 to C7 (table 1). One of these cases was found to have extensive failures in vertebral formation from C3 to T7. Intriguingly, a similar malformation pattern was observed in the *Tbx6*^{up3/up3} mice, in which all of the affected vertebrae were clustered on the cervical segments and no obvious vertebral malformations were observed in the other portions of the spine (figure 5). Among the *Tbx6*^{up3/up3} mice, the incidence of CVMs at the C1 and C2 positions was 55%, and the incidence at the C3 and C4 positions was 10% (figure 5). The shared localization of cervical CVMs in both human subjects and mice with increased *TBX6*/*Tbx6* dosage supports a strong, intrinsic genetic component contributing to this observation. Collectively, our data from human CVM subjects and the mouse model suggest that an increased dosage of *TBX6* or altered developmental expression levels of *Tbx6* increases the risk of CVMs in the cervical vertebrae.

DISCUSSION

Genomic CNVs can be rare variants contributing to human developmental disorders. However, few reports have described the correlation between copy number variants at the *TBX6* locus; i.e. 16p11.2 BP4-BP5 duplication and human CVMs. Here we retrospectively

analyzed the radiological spinal phenotypes of human subjects who were referred to clinical CMA testing and investigated genotype-phenotype correlations. We found that 57% (4/7) of subjects who carried the 16p11.2 BP4-BP5 duplication and that had spinal films available to examine showed CVMs. Meanwhile, our mouse models supported the contention that the increased dosage and expression of *TBX6* may be a major genetic risk factor of CVMs in subjects with 16p11.2 BP4-BP5 duplication. Furthermore, as a member of Ripply family, *RIPPLY2* is a negative regulator of the T-Box family, and bi-allelic mutations in *RIPPLY2* have been reported to be associated with CVMs, consisting of cervical segmentation defects, which may be attributed to the elevated dosage of *TBX6*.^{51,52,53,54} Combined with the genetic evidence in our previous mouse model with decreased *TBX6* dosage,^{14,15} our findings indicated that *TBX6* may act as a morphogen, and unbalanced *TBX6* gene dosage could result in CVMs in both humans and mice.

Due to the frequency of 16p11.2 BP4-BP5 duplication is low in human populations, our single-center based study cannot achieve a large sample size of 16p11.2 BP4-BP5 duplication carriers. Therefore, here we also investigated the previously published data of CVMs and related phenotypes in 16p11.2 BP4-BP5 duplication carriers: 2/10 (20%) in Shinawi et al.,²³ 1/3 (33%) in Fernandez et al.,³⁶ and 1/1 (100%) in Al-Kateb et al.⁷ When combining these previously published data with ours, the overall frequency of CVMs in 16p11.2 BP4-BP5 duplication carriers is 8/21 (38%), which is significantly higher than that observed in two control populations (8/21 VS 19/70747, $P < 0.0001$, OR = 2291, 95% CI: 852 to 6154, by the Fisher's exact test). To further achieve a precise assessment of CVM risks associated with 16p11.2 BP4-BP5 duplication, a large sample size of duplication carriers is required in future studies.

CVMs can occur at any segment of the spine. Generally, from clinical experience human CVMs occur at the thoracic and lumbar segments more commonly than other segments of the spine.¹⁵ Notably, genetic variations in different human genes have been reported to be predictive to the spinal locations of CVMs. Mutations in *MYF5* tend to cause CVMs at cervical vertebrae;⁵⁵ *USP9X* mutations tend to cause CVMs at thoracic vertebrae;⁵⁶ and *FNI* mutations can cause CVMs at thoracic and lumbar vertebrae.⁵⁷ In addition, a gene-dependent distribution of CVMs across the spine has also been proposed in mice. A previous study showed that *Hes7*^{+/-} mice tend to develop CVMs that are mostly located between T7 and L4 vertebrae; *Mesp2*^{+/-} mice tend to be affected with CVMs between T11 and L4 vertebrae; and *Dll1*^{+/-} mice tend to have CVMs between C1 and T2 vertebrae.⁵⁸

In terms of genotype-phenotype correlation with *TBX6*, the CVMs induced by decreased *TBX6* dosage are preferentially localized to the thoracic and lumbar vertebrae in human subjects.^{9,15} Our previous studies and those of others consistently reported the involvement of the 16p11.2 BP4-BP5 deletion or truncating mutations of *TBX6* in human CVMs.^{9,16,17} These subjects are molecularly categorized as TACS (*TBX6*-associated congenital scoliosis), with decreased *TBX6* dosage manifesting hemivertebrae or butterfly vertebrae in the lower half (thoracolumbar or lumbar vertebrae) of the spine (table 1).^{9,14,15} In contrast, here we report that human subjects with an increased dosage of *TBX6* had CVMs localized in the cervical vertebrae, the upper part of the spine (table 1). These findings were recapitulated in the gene-edited mice with increased dosage of *Tbx6* (figure 5). Our experimental

observations provide further evidence of the association between *TBX6* and CVMs (which clinically often manifest as congenital scoliosis), and expand the known phenotypic spectrum of TACS.¹⁵ Considering the gene-deletion and gene-duplication scenarios, our data implicate that divergent *TBX6/Tbx6* gene dosage or expression alterations can result in CVMs at different locations of the spine in both humans and mice.

Currently, it is still challenging to fully explain the molecular mechanism underlying the different localization of CVMs in the spine between the decreased and increased dosages of *TBX6/Tbx6*. The prevailing developmental biology theory of somitogenesis is the clock and wavefront model, which emphasizes that the wave-front from the presomitic mesoderm combines with the clock that drives cells within the same oscillator to differentiate and become parts of the same segment.^{59,60,61} The Wnt and delta-Notch pathways are crucial in modulating the clock and wave-front model.^{60,62} Two independent research groups previously confirmed that Notch signaling is controlled by *Tbx6*, which implicated the importance of *Tbx6* in the process of somitogenesis.^{63,64}

Tbx6 is a member of the T-box gene family,⁶⁵ and formation of the precise border of somites during mouse somitogenesis is determined by the expression of *Tbx6*.⁵² Moreover, formation of the upper part of the spine is different from that of the lower part of the spine, suggesting that a diverse spatiotemporal-regulation pattern occurs during somite development of the upper spine.⁶⁶ Similarly, in chicken embryos, the upper ten somites are molecularly distinct from the lower ones.⁶⁷ The different locations of CVMs among the human cases and the mouse models with different *TBX6/Tbx6* dosages may be attributed to the landscape of differential formation for different parts of the spine. These experimental observations may also result from the potential differences in dosage sensitivity to *Tbx6* across the different vertebral levels of the spine, timing/expression of *Tbx6* downstream genes, or expression gradients transmitting downstream developmental signaling pathways. Due to the complicated nature of the regulatory networks that modulate somitogenesis, further investigations are required to reveal the underlying mechanism for the *TBX6* dosage-dependent localization of CVMs in the spine.

Mouse models generated by genome editing are efficient for studying the genetic contributions to human diseases and genotype-phenotype correlations. The CRISPR-Cas9 technology, an emerging powerful tool for genome editing, can be applied for editing both coding and potential regulatory regions of genes. Upstream conserved regions are likely to be crucial for expression regulation of the associated genes, but may not necessarily be subjected to the same evolutionary constraints as coding exons.⁶⁸ Alterations of these potential regulatory sequences may result in increased or decreased expression of the downstream gene. In this study, we successfully generated mouse mutants with increased *Tbx6* expression and recapitulated the *TBX6* dosage in human carriers of 16p11.2 BP4-BP5 duplication, which can be used in future studies to model the 16p11.2 BP4-BP5 duplication.

In this study, no obvious CVMs were observed in either *Tbx6*^{up1/up1} or *Tbx6*^{up2/up2} mice. We speculate that the mild elevation of *Tbx6* dosage in these two mutants may be insufficient to cause CVMs, which indirectly implicates the dosage-dependent penetrance. Meanwhile, both human subjects with 16p11.2 BP4-BP5 duplication and the *Tbx6*^{up3/up3}

mouse model manifested with increased risks of CVMs, but with incomplete penetrance (i.e., approximately 57% and 60%, respectively). No correlation was observed between this incomplete penetrance and the distribution of *TBX6* hypomorphic alleles (online supplementary figure 6). Therefore, environmental or other factors may be also involved in the pathogenesis and penetrance of CVMs in the 16p11.2 BP4-BP5 duplication carriers. For example, hypoxia can affect somitogenesis and results in vertebral malformations during the embryonic gestational period, and *Tbx6* expression was observed to be decreased under the condition of hypoxia.⁵⁸ Therefore, beyond genetic contributions, environmental factors and other unrecognized perturbations of subtle changes in gene dosage and expression, such as stochastic factors affecting cells in different parts of the body axis, may be involved in the pathogenesis and phenotypic variability of CVMs.

In summary, our experimental observations in both human subjects and mouse models suggest that an increased dosage of *TBX6* among the subjects carrying 16p11.2 BP4-BP5 duplication can induce cervical CVMs. Our findings have implications for clinical diagnosis and genetic counseling for CVMs and other related developmental disorders and for a precision medicine guidance of environmental/therapeutic interventions or avoidance.

Supplementary Material

Refer to Web version on PubMed Central for supplementary material.

Acknowledgments

We would like to thank the families for participating and supporting this study.

Funding

This work was supported by National Natural Science Foundation of China (31571297, 31625015, 31771396, 31521003, 81822030, 81472046, 81772301, 81672123 and 81772299), Shanghai Municipal Science and Technology Major Project (2017SHZDZX01), Shanghai Medical Center of Key Programs for Female Reproductive Diseases (2017ZZ01016), Beijing Natural Science Foundation (7172175), CAMS Initiative Fund for Medical Sciences (2016-I2M-3-003), the US National Institutes of Health, National Institute of Neurological Disorders and Stroke (NINDS R35 NS105078), and the US National Human Genome Research Institute/National Heart Lung and Blood Institute (NHGRI/NHLBI) supported Baylor Hopkins Center for Mendelian Genomics (BHCMG) grant UM1 HG006542.

Competing interests

J.R.L. has stock ownership in 23andMe, is a paid consultant for Regeneron Pharmaceuticals and Novartis, and is a coinventor on multiple United States and European patents related to molecular diagnostics for inherited neuropathies, eye diseases and bacterial genomic fingerprinting. P.L. is an employee of Baylor College of Medicine and derives support through a professional services agreement with Baylor Genetics. The Department of Molecular and Human Genetics at Baylor College of Medicine derives revenue from the chromosomal microarray analysis and clinical exome sequencing offered at Baylor Genetics.

Data sharing statement

All data relevant to the study are included in the article or uploaded as supplementary information.

REFERENCES

1. Giampietro PF, Raggio CL, Blank RD, McCarty C, Broeckel U, Pickart MA. Clinical, genetic and environmental factors associated with congenital vertebral malformations. *Mol Syndromol* 2013;4:94–105. [PubMed: 23653580]
2. Giampietro PF, Dunwoodie SL, Kusumi K, Pourquoi O, Tassy O, Offiah AC, Cornier AS, Alman BA, Blank RD, Raggio CL, Glurich I, Turnpenny PD. Progress in the understanding of the genetic etiology of vertebral segmentation disorders in humans. *Ann N Y Acad Sci* 2009;1151:38–67. [PubMed: 19154516]
3. McMaster MJ, Singh H. Natural history of congenital kyphosis and kyphoscoliosis. A study of one hundred and twelve patients. *J Bone Joint Surg Am* 1999;81:1367–83. [PubMed: 10535587]
4. Wynne-Davies R. Congenital vertebral anomalies: aetiology and relationship to spina bifida cystica. *J Med Genet* 1975;12:280–8. [PubMed: 1100836]
5. Conrad DF, Pinto D, Redon R, Feuk L, Gokcumen O, Zhang Y, Aerts J, Andrews TD, Barnes C, Campbell P, Fitzgerald T, Hu M, Ihm CH, Kristiansson K, Macarthur DG, Macdonald JR, Onyiah I, Pang AW, Robson S, Stirrups K, Valsesia A, Walter K, Wei J, Wellcome Trust Case Control C, Tyler-Smith C, Carter NP, Lee C, Scherer SW, Hurles ME. Origins and functional impact of copy number variation in the human genome. *Nature* 2010;464:704–12. [PubMed: 19812545]
6. Weischenfeldt J, Symmons O, Spitz F, Korbelt JO. Phenotypic impact of genomic structural variation: insights from and for human disease. *Nat Rev Genet* 2013;14:125–38. [PubMed: 23329113]
7. Al-Kateb H, Khanna G, Filges I, Hauser N, Grange DK, Shen J, Smyser CD, Kulkarni S, Shinawi M. Scoliosis and vertebral anomalies: additional abnormal phenotypes associated with chromosome 16p11.2 rearrangement. *Am J Med Genet A* 2014;164A:1118–26. [PubMed: 24458548]
8. Shimojima K, Inoue T, Fujii Y, Ohno K, Yamamoto T. A familial 593-kb microdeletion of 16p11.2 associated with mental retardation and hemivertebrae. *Eur J Med Genet* 2009;52:433–5. [PubMed: 19770079]
9. Wu N, Ming X, Xiao J, Wu Z, Chen X, Shinawi M, Shen Y, Yu G, Liu J, Xie H, Gucev ZS, Liu S, Yang N, Al-Kateb H, Chen J, Zhang J, Hauser N, Zhang T, Tasic V, Liu P, Su X, Pan X, Liu C, Wang L, Shen J, Shen J, Chen Y, Zhang T, Zhang J, Choy KW, Wang J, Wang Q, Li S, Zhou W, Guo J, Wang Y, Zhang C, Zhao H, An Y, Zhao Y, Wang J, Liu Z, Zuo Y, Tian Y, Weng X, Sutton VR, Wang H, Ming Y, Kulkarni S, Zhong TP, Giampietro PF, Dunwoodie SL, Cheung SW, Zhang X, Jin L, Lupski JR, Qiu G, Zhang F. TBX6 null variants and a common hypomorphic allele in congenital scoliosis. *N Engl J Med* 2015;372:341–50. [PubMed: 25564734]
10. Zhang F, Gu W, Hurles ME, Lupski JR. Copy number variation in human health, disease, and evolution. *Annu Rev Genomics Hum Genet* 2009;10:451–81. [PubMed: 19715442]
11. Almal SH, Padh H. Implications of gene copy-number variation in health and diseases. *J Hum Genet* 2012;57:6–13. [PubMed: 21956041]
12. Zarrei M, MacDonald JR, Merico D, Scherer SW. A copy number variation map of the human genome. *Nat Rev Genet* 2015;16:172–83. [PubMed: 25645873]
13. Rice AM, McLysaght A. Dosage-sensitive genes in evolution and disease. *BMC Biol* 2017;15:78. [PubMed: 28863777]
14. Yang N, Wu N, Zhang L, Zhao Y, Liu J, Liang X, Ren X, Li W, Chen W, Dong S, Zhao S, Lin J, Xiang H, Xue H, Chen L, Sun H, Zhang J, Shi J, Zhang S, Lu D, Wu X, Jin L, Ding J, Qiu G, Wu Z, Lupski JR, Zhang F. TBX6 compound inheritance leads to congenital vertebral malformations in humans and mice. *Hum Mol Genet* 2019;28:539–47. [PubMed: 30307510]
15. Liu J, Wu N, Yang N, Takeda K, Chen W, Li W, Du R, Liu S, Zhou Y, Zhang L, Liu Z, Zuo Y, Zhao S, Blank R, Pehlivan D, Dong S, Zhang J, Shen J, Si N, Wang Y, Liu G, Li S, Zhao Y, Zhao H, Chen Y, Zhao Y, Song X, Hu J, Lin M, Tian Y, Yuan B, Yu K, Niu Y, Yu B, Li X, Chen J, Yan Z, Zhu Q, Meng X, Chen X, Su J, Zhao X, Wang X, Ming Y, Li X, Raggio CL, Zhang B, Weng X, Zhang S, Zhang X, Watanabe K, Matsumoto M, Jin L, Shen Y, Sobreira NL, Posey JE, Giampietro PF, Valle D, Liu P, Wu Z, Ikegawa S, Lupski JR, Zhang F, Qiu G. TBX6-associated congenital scoliosis (TACS) as a clinically distinguishable subtype of congenital scoliosis: further evidence supporting the compound inheritance and TBX6 gene dosage model. *Genet Med* 2019;21:1548–58. [PubMed: 30636772]

16. Lefebvre M, Duffourd Y, Jouan T, Poe C, Jean-Marcais N, Verloes A, St-Onge J, Riviere JB, Petit F, Pierquin G, Demeer B, Callier P, Thauvin-Robinet C, Faivre L, Thevenon J. Autosomal recessive variations of TBX6, from congenital scoliosis to spondylocostal dysostosis. *Clin Genet* 2017;91:908–12. [PubMed: 27861764]
17. Takeda K, Kou I, Kawakami N, Iida A, Nakajima M, Ogura Y, Imagawa E, Miyake N, Matsumoto N, Yasuhiko Y, Sudo H, Kotani T, Japan Early Onset Scoliosis Research G, Nakamura M, Matsumoto M, Watanabe K, Ikegawa S. Compound Heterozygosity for Null Mutations and a Common Hypomorphic Risk Haplotype in TBX6 Causes Congenital Scoliosis. *Hum Mutat* 2017;38:317–23. [PubMed: 28054739]
18. Nuttle X, Giannuzzi G, Duyzend MH, Schraiber JG, Narvaiza I, Sudmant PH, Penn O, Chiatante G, Malig M, Huddleston J, Benner C, Camponeschi F, Ciofi-Baffoni S, Stessman HA, Marchetto MC, Denman L, Harshman L, Baker C, Raja A, Penewit K, Janke N, Tang WJ, Ventura M, Banci L, Antonacci F, Akey JM, Amemiya CT, Gage FH, Reymond A, Eichler EE. Emergence of a Homo sapiens-specific gene family and chromosome 16p11.2 CNV susceptibility. *Nature* 2016;536:205–9. [PubMed: 27487209]
19. Zufferey F, Sherr EH, Beckmann ND, Hanson E, Maillard AM, Hippolyte L, Mace A, Ferrari C, Kutalik Z, Andrieux J, Aylward E, Barker M, Bernier R, Bouquillon S, Conus P, Delobel B, Faucett W, Goin-Kochel RP, Grant E, Harewood L, Hunter JV, Lebon S, Ledbetter DH, Martin CL, Mannik K, Martinet D, Mukherjee P, Ramocki MB, Spence SJ, Steinman KJ, Tjernagel J, Spiro JE, Reymond A, Beckmann JS, Chung WK, Jacquemont S, Consortium SV, Consortium P-E. A 600 kb deletion syndrome at 16p11.2 leads to energy imbalance and neuropsychiatric disorders. *J Med Genet* 2012;49:660–8. [PubMed: 23054248]
20. Jacquemont S, Reymond A, Zufferey F, Harewood L, Walters RG, Kutalik Z, Martinet D, Shen Y, Valsesia A, Beckmann ND, Thorleifsson G, Belfiore M, Bouquillon S, Champion D, de Leeuw N, de Vries BB, Esko T, Fernandez BA, Fernandez-Aranda F, Fernandez-Real JM, Gratacos M, Guilmatre A, Hoyer J, Jarvelin MR, Kooy RF, Kurg A, Le Caignec C, Mannik K, Platt OS, Sanlaville D, Van Haelst MM, Villatoro Gomez S, Walha F, Wu BL, Yu Y, Aboura A, Addor MC, Alembik Y, Antonarakis SE, Arveiler B, Barth M, Bednarek N, Bena F, Bergmann S, Beri M, Bernardini L, Blaumeiser B, Bonneau D, Bottani A, Boute O, Brunner HG, Cailley D, Callier P, Chiesa J, Chrast J, Coin L, Coutton C, Cuisset JM, Cuvellier JC, David A, de Freminville B, Delobel B, Delrue MA, Demeer B, Descamps D, Didelot G, Dieterich K, Disciglio V, Doco-Fenzy M, Drunat S, Duban-Bedu B, Dubourg C, El-Sayed Moustafa JS, Elliott P, Faas BH, Faivre L, Faudet A, Fellmann F, Ferrarini A, Fisher R, Flori E, Forer L, Gaillard D, Gerard M, Gieger C, Gimelli S, Gimelli G, Grabe HJ, Guichet A, Guillin O, Hartikainen AL, Heron D, Hippolyte L, Holder M, Homuth G, Isidor B, Jaillard S, Jaros Z, Jimenez-Murcia S, Helas GJ, Jonveaux P, Kaksonen S, Keren B, Kloss-Brandstatter A, Knoers NV, Koolen DA, Kroisel PM, Kronenberg F, Labalme A, Landais E, Lapi E, Layet V, Legallic S, Leheup B, Leube B, Lewis S, Lucas J, MacDermot KD, Magnusson P, Marshall C, Mathieu-Dramard M, McCarthy MI, Meitinger T, Mencarelli MA, Merla G, Moerman A, Mooser V, Morice-Picard F, Mucciolo M, Nauck M, Ndiaye NC, Nordgren A, Pasquier L, Petit F, Pfundt R, Plessis G, Rajcan-Separovic E, Ramelli GP, Rauch A, Ravazzolo R, Reis A, Renieri A, Richart C, Ried JS, Rieubland C, Roberts W, Roetzer KM, Rooryck C, Rossi M, Saemundsen E, Satre V, Schurmann C, Sigurdsson E, Stavropoulos DJ, Stefansson H, Tengstrom C, Thorsteinsdottir U, Tinahones FJ, Touraine R, Vallee L, van Binsbergen E, Van der Aa N, Vincent-Delorme C, Visvikis-Siest S, Vollenweider P, Volzke H, Vulto-van Silfhout AT, Waeber G, Wallgren-Pettersson C, Witwicki RM, Zwolinski S, Andrieux J, Estivill X, Gusella JF, Gustafsson O, Metspalu A, Scherer SW, Stefansson K, Blakemore AI, Beckmann JS, Froguel P. Mirror extreme BMI phenotypes associated with gene dosage at the chromosome 16p11.2 locus. *Nature* 2011;478:97–102. [PubMed: 21881559]
21. Moreno-De-Luca A, Evans DW, Boomer KB, Hanson E, Bernier R, Goin-Kochel RP, Myers SM, Challman TD, Moreno-De-Luca D, Slane MM, Hare AE, Chung WK, Spiro JE, Faucett WA, Martin CL, Ledbetter DH. The role of parental cognitive, behavioral, and motor profiles in clinical variability in individuals with chromosome 16p11.2 deletions. *JAMA Psychiat* 2015;72:119–26.
22. Lupski JR. 2018 Victor A. McKusick Leadership Award: Molecular Mechanisms for Genomic and Chromosomal Rearrangements. *Am J Hum Genet* 2019;104:391–406. [PubMed: 30849326]
23. Shinawi M, Liu P, Kang SH, Shen J, Belmont JW, Scott DA, Probst FJ, Craigen WJ, Graham BH, Pursley A, Clark G, Lee J, Proud M, Stocco A, Rodriguez DL, Kozel BA, Sparagana S,

- Roeder ER, McGrew SG, Kurczynski TW, Allison LJ, Amato S, Savage S, Patel A, Stankiewicz P, Beaudet AL, Cheung SW, Lupski JR. Recurrent reciprocal 16p11.2 rearrangements associated with global developmental delay, behavioural problems, dysmorphism, epilepsy, and abnormal head size. *J Med Genet* 2010;47:332–41. [PubMed: 19914906]
24. Walters RG, Jacquemont S, Valsesia A, de Smith AJ, Martinet D, Andersson J, Falchi M, Chen F, Andrieux J, Lobbens S, Delobel B, Stutzmann F, Moustafa JSES, Chevre JC, Lecoeur C, Vatin V, Bouquillon S, Buxton JL, Boute O, Holder-Espinasse M, Cuisset JM, Lemaitre MP, Ambresin AE, Brioschi A, Gaillard M, Giusti V, Fellmann F, Ferrarini A, Hadjikhani N, Campion D, Guilmatre A, Goldenberg A, Calmels N, Mandel JL, Le Caignec C, David A, Isidor B, Cordier MP, Dupuis-Girod S, Labalme A, Sanlaville D, Beri-Dexheimer M, Jonveaux P, Leheup B, Ounap K, Bochukova EG, Henning E, Keogh J, Ellis RJ, MacDermot KD, van Haelst MM, Vincent-Delorme C, Plessis G, Touraine R, Philippe A, Malan V, Mathieu-Dramard M, Chiesa J, Blaumeiser B, Kooy RF, Caiazzo R, Pigeyre M, Balkau B, Sladek R, Bergmann S, Mooser V, Waterworth D, Reymond A, Vollenweider P, Waeber G, Kurg A, Palta P, Esko T, Metspalu A, Nelis M, Elliott P, Hartikainen AL, McCarthy MI, Peltonen L, Carlsson L, Jacobson P, Sjostrom L, Huang N, Hurler ME, O'Rahilly S, Farooqi IS, Mannik K, Jarvelin MR, Pattou F, Meyre D, Walley AJ, Coin LJM, Blakemore AIF, Froguel P, Beckmann JS. A new highly penetrant form of obesity due to deletions on chromosome 16p11.2. *Nature* 2010;463:671–U104. [PubMed: 20130649]
 25. Qureshi AY, Mueller S, Snyder AZ, Mukherjee P, Berman JI, Roberts TP, Nagarajan SS, Spiro JE, Chung WK, Sherr EH, Buckner RL. Opposing brain differences in 16p11.2 deletion and duplication carriers. *J Neurosci* 2014;34:11199–211. [PubMed: 25143601]
 26. Maillard AM, Ruef A, Pizzagalli F, Migliavacca E, Hippolyte L, Adaszewski S, Dukart J, Ferrari C, Conus P, Mannik K, Zazhytska M, Siffredi V, Maeder P, Kutalik Z, Kherif F, Hadjikhani N, Beckmann JS, Reymond A, Draganski B, Jacquemont S, p11.2 European C. The 16p11.2 locus modulates brain structures common to autism, schizophrenia and obesity. *Mol Psychiatry* 2015;20:140–7.
 27. Martin-Brevet S, Rodriguez-Herreros B, Nielsen JA, Moreau C, Modenato C, Maillard AM, Pain A, Richetin S, Jonch AE, Qureshi AY, Zurcher NR, Conus P, p11.2 European C, Simons Variation in Individuals Project C, Chung WK, Sherr EH, Spiro JE, Kherif F, Beckmann JS, Hadjikhani N, Reymond A, Buckner RL, Draganski B, Jacquemont S. Quantifying the Effects of 16p11.2 Copy Number Variants on Brain Structure: A Multisite Genetic-First Study. *Biol Psychiatry* 2018;84:253–64. [PubMed: 29778275]
 28. Qiu Y, Arbogast T, Lorenzo SM, Li H, Tang SC, Richardson E, Hong O, Cho S, Shanta O, Pang T, Corsello C, Deutsch CK, Chevalier C, Davis EE, Iakoucheva LM, Herault Y, Katsanis N, Messer K, Sebat J. Oligogenic Effects of 16p11.2 Copy-Number Variation on Craniofacial Development. *Cell Rep* 2019;28:3320–8 e4. [PubMed: 31553903]
 29. Weiss LA, Shen Y, Korn JM, Arking DE, Miller DT, Fossdal R, Saemundsen E, Stefansson H, Ferreira MA, Green T, Platt OS, Ruderfer DM, Walsh CA, Altshuler D, Chakravarti A, Tanzi RE, Stefansson K, Santangelo SL, Gusella JF, Sklar P, Wu BL, Daly MJ. Association between microdeletion and microduplication at 16p11.2 and autism. *N Engl J Med* 2008;358:667–75. [PubMed: 18184952]
 30. McCarthy SE, Makarov V, Kirov G, Addington AM, McClellan J, Yoon S, Perkins DO, Dickel DE, Kusenda M, Krastoshevsky O, Krause V, Kumar RA, Grozeva D, Malhotra D, Walsh T, Zackai EH, Kaplan P, Ganesh J, Krantz ID, Spinner NB, Roccanova P, Bhandari A, Pavon K, Lakshmi B, Leotta A, Kendall J, Lee YH, Vacic V, Gary S, Iakoucheva LM, Crow TJ, Christian SL, Lieberman JA, Stroup TS, Lehtimaki T, Puura K, Haldeman-Englert C, Pearl J, Goodell M, Willour VL, Derosse P, Steele J, Kassem L, Wolff J, Chitkara N, McMahon FJ, Malhotra AK, Potash JB, Schulze TG, Nothen MM, Cichon S, Rietschel M, Leibenluft E, Kustanovich V, Lajonchere CM, Sutcliffe JS, Skuse D, Gill M, Gallagher L, Mendell NR, Craddock N, Owen MJ, O'Donovan MC, Shaikh TH, Susser E, Delisi LE, Sullivan PF, Deutsch CK, Rapoport J, Levy DL, King MC, Sebat J. Microduplications of 16p11.2 are associated with schizophrenia. *Nat Genet* 2009;41:1223–7. [PubMed: 19855392]
 31. Blumenthal I, Ragavendran A, Erdin S, Klei L, Sugathan A, Guide JR, Manavalan P, Zhou JQ, Wheeler VC, Levin JZ, Ernst C, Roeder K, Devlin B, Gusella JF, Talkowski ME. Transcriptional

- consequences of 16p11.2 deletion and duplication in mouse cortex and multiplex autism families. *Am J Hum Genet* 2014;94:870–83. [PubMed: 24906019]
32. Horev G, Ellegood J, Lerch JP, Son YEE, Muthuswamy L, Vogel H, Krieger AM, Buja A, Henkelman RM, Wigler M, Mills AA. Dosage-dependent phenotypes in models of 16p11.2 lesions found in autism. *P Natl Acad Sci U S A* 2011;108:17076–81.
 33. Arbogast T, Ouagazzal AM, Chevalier C, Kopanitsa M, Afinowi N, Migliavacca E, Cowling BS, Birling MC, Champy MF, Reymond A, Hérault Y. Reciprocal Effects on Neurocognitive and Metabolic Phenotypes in Mouse Models of 16p11.2 Deletion and Duplication Syndromes. *PLoS Genet* 2016;12:e1005709. [PubMed: 26872257]
 34. Walz K, Paylor R, Yan J, Bi W, Lupski JR. Rai1 duplication causes physical and behavioral phenotypes in a mouse model of dup(17)(p11.2p11.2). *J Clin Invest* 2006;116:3035–41. [PubMed: 17024248]
 35. Ricard G, Molina J, Chrast J, Gu W, Gheldof N, Pradervand S, Schutz F, Young JI, Lupski JR, Reymond A, Walz K. Phenotypic consequences of copy number variation: insights from Smith-Magenis and Potocki-Lupski syndrome mouse models. *PLoS Biol* 2010;8:e1000543. [PubMed: 21124890]
 36. Fernandez BA, Roberts W, Chung B, Weksberg R, Meyn S, Szatmari P, Joseph-George AM, Mackay S, Whitten K, Noble B, Vardy C, Crosbie V, Luscombe S, Tucker E, Turner L, Marshall CR, Scherer SW. Phenotypic spectrum associated with de novo and inherited deletions and duplications at 16p11.2 in individuals ascertained for diagnosis of autism spectrum disorder. *J Med Genet* 2010;47:195–203. [PubMed: 19755429]
 37. D'Angelo D, Lebon S, Chen Q, Martin-Brevet S, Snyder LG, Hippolyte L, Hanson E, Maillard AM, Faucett WA, Mace A, Pain A, Bernier R, Chawner SJ, David A, Andrieux J, Aylward E, Baujat G, Caldeira I, Conus P, Ferrari C, Forzano F, Gerard M, Goin-Kochel RP, Grant E, Hunter JV, Isidor B, Jacqueline A, Jonch AE, Keren B, Lacombe D, Le Caignec C, Martin CL, Mannik K, Metspalu A, Mignot C, Mukherjee P, Owen MJ, Passeggeri M, Rooryck-Thambo C, Rosenfeld JA, Spence SJ, Steinman KJ, Tjernagel J, Van Haelst M, Shen Y, Draganski B, Sherr EH, Ledbetter DH, van den Bree MB, Beckmann JS, Spiro JE, Reymond A, Jacquemont S, Chung WK, Cardiff University Experiences of Children With Copy Number Variants S, p11.2 European C, Simons Variation in Individuals Project C. Defining the Effect of the 16p11.2 Duplication on Cognition, Behavior, and Medical Comorbidities. *JAMA Psychiat* 2016;73:20–30.
 38. Ou Z, Kang SH, Shaw CA, Carmack CE, White LD, Patel A, Beaudet AL, Cheung SW, Chinault AC. Bacterial artificial chromosome-emulation oligonucleotide arrays for targeted clinical array-comparative genomic hybridization analyses. *Genet Med* 2008;10:278–89. [PubMed: 18414211]
 39. Shaw CJ, Shaw CA, Yu W, Stankiewicz P, White LD, Beaudet AL, Lupski JR. Comparative genomic hybridisation using a proximal 17p BAC/PAC array detects rearrangements responsible for four genomic disorders. *J Med Genet* 2004;41:113–9. [PubMed: 14757858]
 40. Cheung SW, Shaw CA, Yu W, Li J, Ou Z, Patel A, Yatsenko SA, Cooper ML, Furman P, Stankiewicz P, Lupski JR, Chinault AC, Beaudet AL. Development and validation of a CGH microarray for clinical cytogenetic diagnosis. *Genet Med* 2005;7:422–32. [PubMed: 16024975]
 41. Ran FA, Hsu PD, Wright J, Agarwala V, Scott DA, Zhang F. Genome engineering using the CRISPR-Cas9 system. *Nat Protoc* 2013;8:2281–308. [PubMed: 24157548]
 42. Platt RJ, Chen S, Zhou Y, Yim MJ, Swiech L, Kempton HR, Dahlman JE, Parnas O, Eisenhaure TM, Jovanovic M, Graham DB, Jhunjhunwala S, Heidenreich M, Xavier RJ, Langer R, Anderson DG, Hacohen N, Regev A, Feng G, Sharp PA, Zhang F. CRISPR-Cas9 knockin mice for genome editing and cancer modeling. *Cell* 2014;159:440–55. [PubMed: 25263330]
 43. Habara-Ohkubo A Differentiation of beating cardiac muscle cells from a derivative of P19 embryonal carcinoma cells. *Cell Struct Funct* 1996;21:101–10. [PubMed: 8790939]
 44. Gavrilov S, Nuhrenberg TG, Ashton AW, Peng CF, Moore JC, Konstantinidis K, Mummery CL, Kitsis RN. Tbx6 is a determinant of cardiac and neural cell fate decisions in multipotent P19CL6 cells. *Differentiation* 2012;84:176–84. [PubMed: 22721678]
 45. Saga Y, Hata N, Kobayashi S, Magnuson T, Seldin MF, Taketo MM. MesP1: a novel basic helix-loop-helix protein expressed in the nascent mesodermal cells during mouse gastrulation. *Development* 1996;122:2769–78. [PubMed: 8787751]

46. Grau C, Starkovich M, Azamian MS, Xia F, Cheung SW, Evans P, Henderson A, Lalani SR, Scott DA. Xp11.22 deletions encompassing CENPV1, CENPV2, MAGED1 and GSPT2 as a cause of syndromic X-linked intellectual disability. *PLoS One* 2017;12:e0175962. [PubMed: 28414775]
47. Bi W, Cheung SW, Breman AM, Bacino CA. 4p16.3 microdeletions and microduplications detected by chromosomal microarray analysis: New insights into mechanisms and critical regions. *Am J Med Genet A* 2016;170:2540–50. [PubMed: 27287194]
48. Daruwalla JS, Balasubramaniam P, Chay SO, Rajan U, Lee HP. Idiopathic scoliosis. Prevalence and ethnic distribution in Singapore schoolchildren. *J Bone Joint Surg Br* 1985;67:182–4. [PubMed: 3980521]
49. Deshpande A, Yadav S, Dao DQ, Wu ZY, Hokanson KC, Cahill MK, Wiita AP, Jan YN, Ullian EM, Weiss LA. Cellular Phenotypes in Human iPSC-Derived Neurons from a Genetic Model of Autism Spectrum Disorder. *Cell Rep* 2017;21:2678–87. [PubMed: 29212016]
50. Chapman DL, Agulnik I, Hancock S, Silver LM, Papaioannou VE. Tbx6, a mouse T-Box gene implicated in paraxial mesoderm formation at gastrulation. *Dev Biol* 1996;180:534–42. [PubMed: 8954725]
51. McInerney-Leo AM, Sparrow DB, Harris JE, Gardiner BB, Marshall MS, O'Reilly VC, Shi H, Brown MA, Leo PJ, Zankl A, Dunwoodie SL, Duncan EL. Compound heterozygous mutations in RIPPLY2 associated with vertebral segmentation defects. *Hum Mol Genet* 2015;24:1234–42. [PubMed: 25343988]
52. Zhao W, Ajima R, Ninomiya Y, Saga Y. Segmental border is defined by Ripply2-mediated Tbx6 repression independent of Mesp2. *Dev Biol* 2015;400:105–17. [PubMed: 25641698]
53. Kawamura A, Koshida S, Takada S. Activator-to-repressor conversion of T-box transcription factors by the Ripply family of Groucho/TLE-associated mediators. *Mol Cell Biol* 2008;28:3236–44. [PubMed: 18332117]
54. Karaca E, Yuregir OO, Bozdogan ST, Aslan H, Pehlivan D, Jhangiani SN, Akdemir ZC, Gambin T, Bayram Y, Atik MM, Erdin S, Muzny D, Gibbs RA, Lupski JR, Baylor-Hopkins Center for Mendelian G. Rare variants in the notch signaling pathway describe a novel type of autosomal recessive Klippel-Feil syndrome. *Am J Med Genet A* 2015;167A:2795–9. [PubMed: 26238661]
55. Di Gioia SA, Shaaban S, Tuysuz B, Elcioglu NH, Chan WM, Robson CD, Ecklund K, Gillette NM, Hamzaoglu A, Tayfun GA, Traboulsi EI, Engle EC. Recessive MYF5 Mutations Cause External Ophthalmoplegia, Rib, and Vertebral Anomalies. *Am J Hum Genet* 2018;103:115–24. [PubMed: 29887215]
56. Reijnders MR, Zachariadis V, Latour B, Jolly L, Mancini GM, Pfundt R, Wu KM, van Ravenswaaij-Arts CM, Veenstra-Knol HE, Anderlid BM, Wood SA, Cheung SW, Barnicoat A, Probst F, Magoulas P, Brooks AS, Malmgren H, Harila-Saari A, Marcelis CM, Vreeburg M, Hobson E, Sutton VR, Stark Z, Vogt J, Cooper N, Lim JY, Price S, Lai AH, Domingo D, Reversade B, Study DDD, Gecz J, Gilissen C, Brunner HG, Kini U, Roepman R, Nordgren A, Kleefstra T. De Novo Loss-of-Function Mutations in USP9X Cause a Female-Specific Recognizable Syndrome with Developmental Delay and Congenital Malformations. *Am J Hum Genet* 2016;98:373–81. [PubMed: 26833328]
57. Lee CS, Fu H, Baratang N, Rousseau J, Kumra H, Sutton VR, Niceta M, Ciolfi A, Yamamoto G, Bertola D, Marcelis CL, Lugtenberg D, Bartuli A, Kim C, Hoover-Fong J, Sobreira N, Pauli R, Bacino C, Krakow D, Parboosingh J, Yap P, Kariminejad A, McDonald MT, Aracena MI, Lausch E, Unger S, Superti-Furga A, Lu JT, Baylor-Hopkins Center for Mendelian G, Cohn DH, Tartaglia M, Lee BH, Reinhardt DP, Campeau PM. Mutations in Fibronectin Cause a Subtype of Spondylometaphyseal Dysplasia with “Corner Fractures”. *Am J Hum Genet* 2017;101:815–23. [PubMed: 29100092]
58. Sparrow DB, Chapman G, Smith AJ, Mattar MZ, Major JA, O'Reilly VC, Saga Y, Zackai EH, Dormans JP, Alman BA, McGregor L, Kageyama R, Kusumi K, Dunwoodie SL. A mechanism for gene-environment interaction in the etiology of congenital scoliosis. *Cell* 2012;149:295–306. [PubMed: 22484060]
59. Cooke J, Zeeman EC. A clock and wavefront model for control of the number of repeated structures during animal morphogenesis. *J Theor Biol* 1976;58:455–76. [PubMed: 940335]

60. Oates AC, Morelli LG, Ares S. Patterning embryos with oscillations: structure, function and dynamics of the vertebrate segmentation clock. *Development* 2012;139:625–39. [PubMed: 22274695]
61. Dequeant ML, Glynn E, Gaudenz K, Wahl M, Chen J, Mushegian A, Pourquie O. A complex oscillating network of signaling genes underlies the mouse segmentation clock. *Science* 2006;314:1595–8. [PubMed: 17095659]
62. Krol AJ, Roellig D, Dequeant ML, Tassy O, Glynn E, Hattem G, Mushegian A, Oates AC, Pourquie O. Evolutionary plasticity of segmentation clock networks. *Development* 2011;138:2783–92. [PubMed: 21652651]
63. Hofmann M, Schuster-Gossler K, Watabe-Rudolph M, Aulehla A, Herrmann BG, Gossler A. WNT signaling, in synergy with T/TBX6, controls Notch signaling by regulating Dll1 expression in the presomitic mesoderm of mouse embryos. *Genes Dev* 2004;18:2712–7. [PubMed: 15545628]
64. Yasuhiko Y, Haraguchi S, Kitajima S, Takahashi Y, Kanno J, Saga Y. Tbx6-mediated Notch signaling controls somite-specific Mesp2 expression. *Proc Natl Acad Sci U S A* 2006;103:3651–6. [PubMed: 16505380]
65. Goering LM, Hoshijima K, Hug B, Bisgrove B, Kispert A, Grunwald DJ. An interacting network of T-box genes directs gene expression and fate in the zebrafish mesoderm. *Proc Natl Acad Sci U S A* 2003;100:9410–5. [PubMed: 12883008]
66. Maschner A, Kruck S, Draga M, Prols F, Scaal M. Developmental dynamics of occipital and cervical somites. *J Anat* 2016;229:601–9. [PubMed: 27380812]
67. Rodrigues S, Santos J, Palmeirim I. Molecular characterization of the rostral-most somites in early somitic stages of the chick embryo. *Gene Expr Patterns* 2006;6:673–7. [PubMed: 16488196]
68. Singal DP, Qiu X. Polymorphism in the upstream regulatory region and level of expression of HLA-DRB genes. *Mol Immunol* 1994;31:1117–20. [PubMed: 7523867]

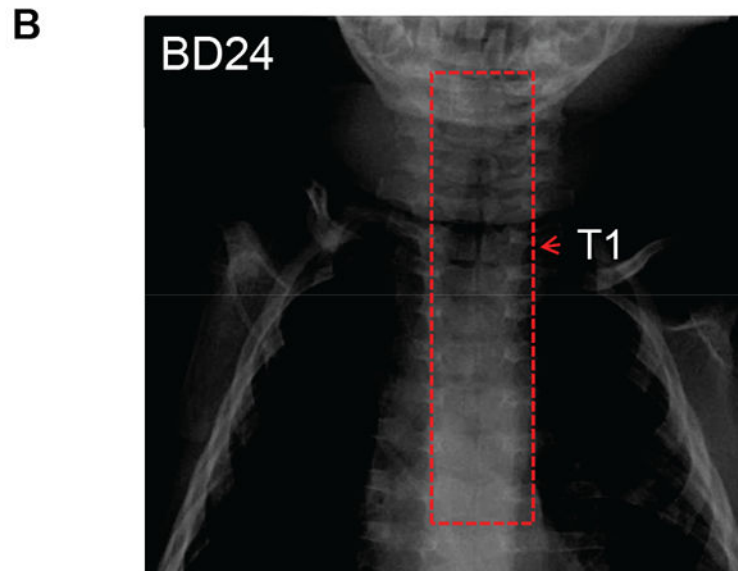
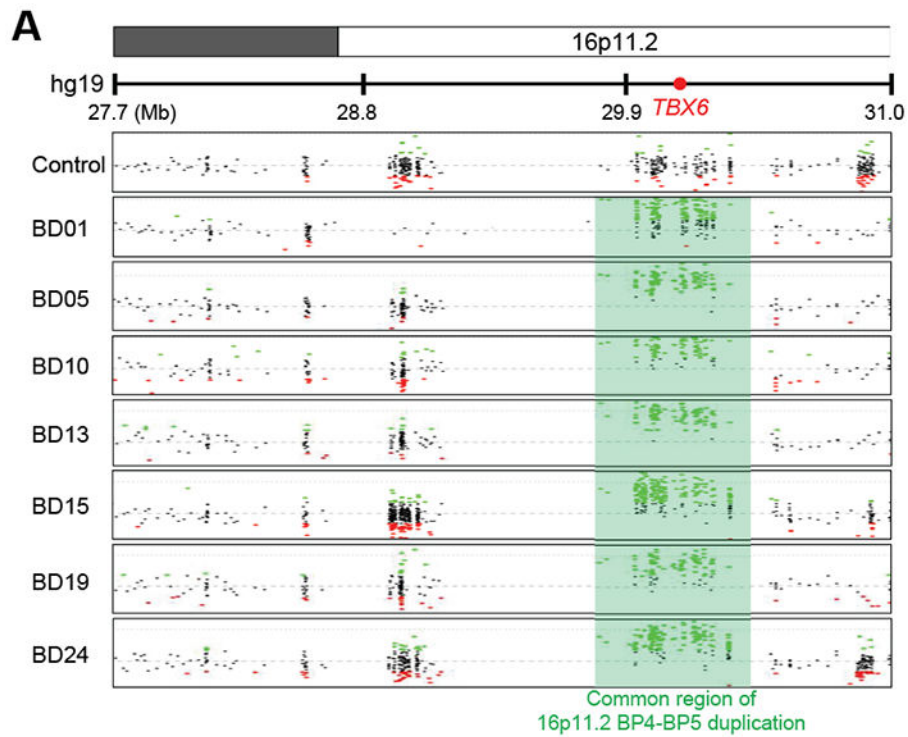
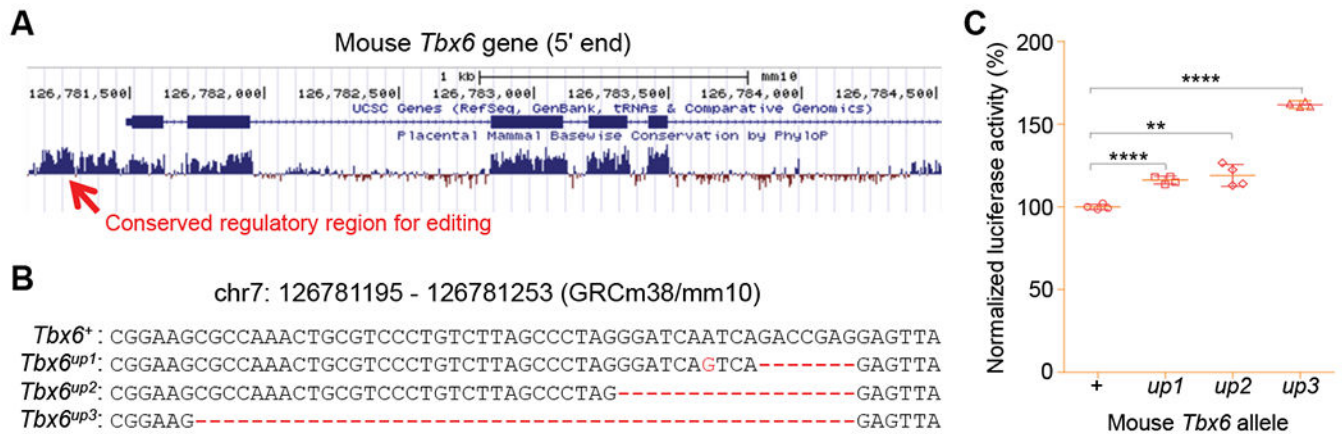


Figure 1. Human subjects with 16p11.2 BP4-BP5 duplication. **(A)** 16p11.2 BP4-BP5 duplications (highlighted with a green box) were confirmed in seven human subjects by CMA. Different versions of CMA microarrays were applied to these individuals. **(B)** The spinal X-ray results of subject BD24 were exemplified. Extensive defects of the vertebral plates from C3 to T7 (red rectangle) were observed in subject BD24 with 16p11.2 BP4-BP5 duplication.

**Figure 2.**

Genetic editing of the conserved upstream region of mouse *Tbx6* results in elevated *Tbx6* expression. (A) The targeted region for genome editing is indicated with a red arrow. (B) The mutated non-coding sequences of three *Tbx6* mutants (*up1*, *up2*, and *up3*) with elevated *Tbx6* expression. Genome editing was conducted using the CRISPR-Cas9 technology in the target region of mouse *Tbx6*. The deleted sequences are indicated with red dashed lines. The mutated nucleotides are shown in red. (C) The elevated expression of *Tbx6* in three mutants was investigated *in vitro* using the luciferase reporter assay in P19CL6 cells. Each assay was performed with at least three replicates. The *Tbx6*^{up3} allele showed an elevated *Tbx6* expression level of approximately 160% of that in the wild-type allele. **, $P < 0.01$; ****, $P < 0.0001$. Abbreviation: “up”, up-regulation.

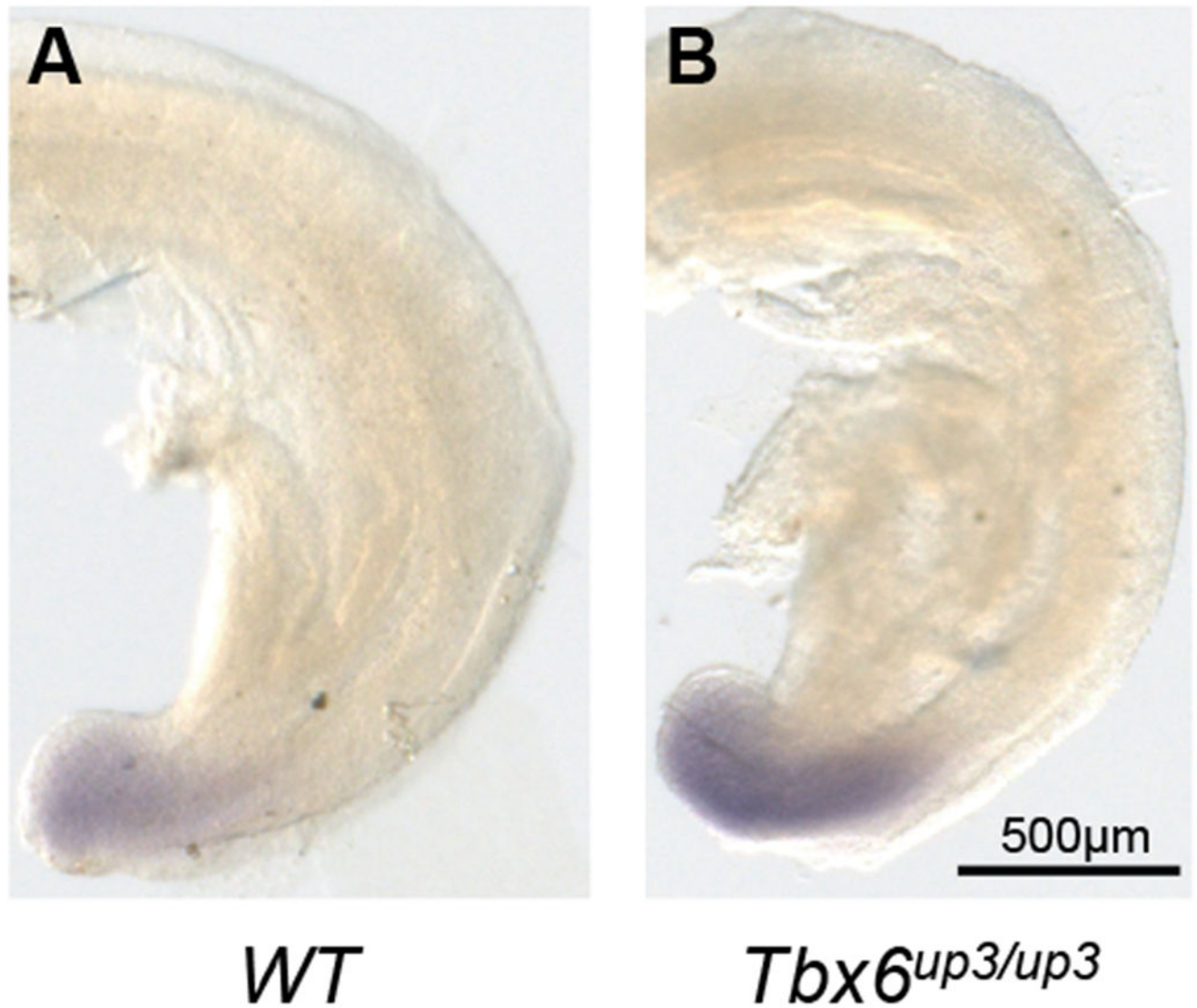


Figure 3.

The elevated expression level of *Tbx6* in the *Tbx6*^{up3/up3} mice was confirmed using whole-mount RNA *in situ* hybridization assays in embryos. The wild-type (*WT*, **A**) and *Tbx6*^{up3/up3} E9.5 embryos (**B**) are shown. The light purple signals at the caudal side of mouse embryos indicate the transcription of *Tbx6*. *Tbx6* transcription was higher in the *Tbx6*^{up3/up3} embryos than in the wild-type embryos.

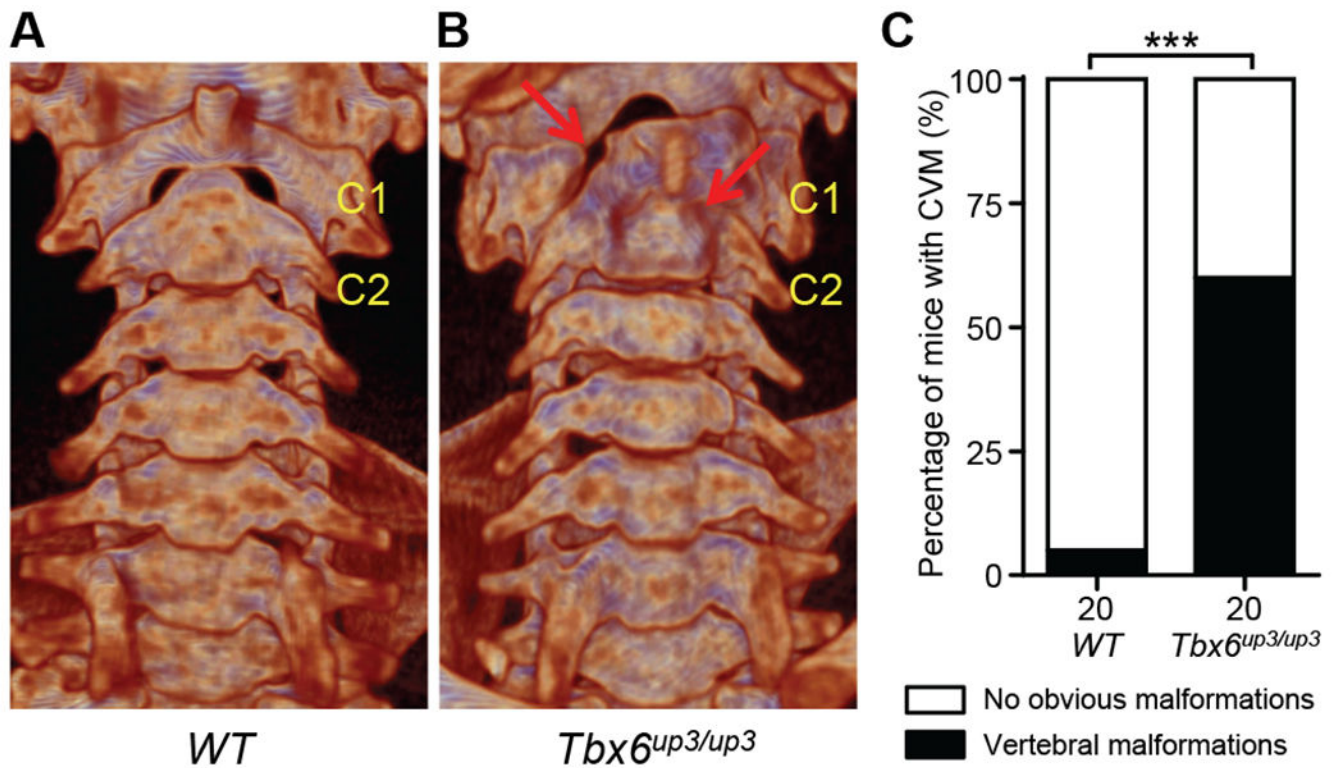


Figure 4. Micro-CT analysis of vertebrae in the *WT* and *Tbx6^{up3/up3}* mice. (A) *WT* mice. (B) *Tbx6^{up3/up3}* mice manifested with CVMs, including cervical fusions and vertebral clefts (red arrow). (C) The rate of CVMs is 60% in *Tbx6^{up3/up3}* mice. Sample sizes are shown below each column. The mice in each group were age- and sex-matched.

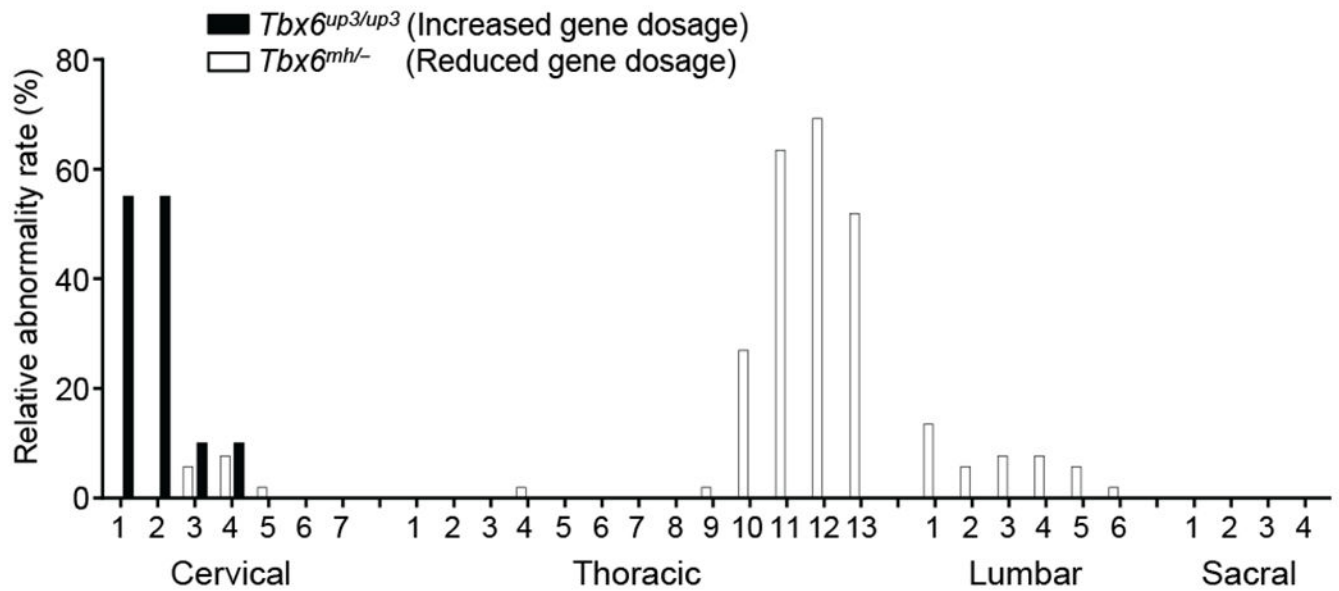


Figure 5.

Divergent distributions of vertebral malformations in the mouse models of increased versus reduced expressions of *Tbx6*. The X-axis shows the vertebral distribution of CVMs in the spine, and the Y-axis shows the abnormality rate in each vertebra. The *Tbx6^{mh/-}* mice, which showed reduced *Tbx6* expression, presented with vertebral malformations mainly in thoracic and lumbar vertebrae, as previously described.¹⁵ The *Tbx6^{up3/up3}* mice, which showed increased *Tbx6* expression, presented with cervical vertebral malformations. The sample sizes of *Tbx6^{mh/-}* and *Tbx6^{up3/up3}* mice are 52 and 20, respectively.

Table 1

Vertebral evaluation of human subjects with 16p11.2 BP4-BP5 duplications

Human subject	Ancestry	Sex	Age ^a	16p11.2 BP4-BP5 CNV	Vertebral malformations ^b
BD01	NHW	M	16 y	duplication	Failure of formation of C6 and C7, cleft of the vertebral plate of C7
BD05	NHW	M	8 y	duplication	Failure of formation of C6 and C7
BD10	NHW	F	4 y	duplication	Normal
BD13	NHW	M	14 y	duplication	Failure of formation of C5 and C6
BD15	NHW	M	1 y	duplication	Normal
BD19	NHW	F	10 m	duplication	Normal
BD24	NHW	M	9 m	duplication	Extensive failure of formation of vertebral plate from C3 to T7
Deletion controls ^c	2 Caucasian, 2 Hispanic	3F, 1M	NA	deletion	4/12 deletion carrier manifest with hemivertebrae at thoracic or thoracolumbar vertebrae

Abbreviations: F, female; M, male; NHW, non-Hispanic (White); NA, not available.

^a y, denotes "year(s) old"; m, denotes "months old".^b C₁, denotes cervical vertebrae; T₁, denotes thoracic vertebrae.^c These data of control deletion carriers have been published in our previous studies.^{9,15}